ization,[1] only small differences can exist between the relative energies of the transition states for the formation of the two isomers. The benzyl group would be expected to have small steric effects in the proposed transition state. However, if the monomer, $(CH_3)_2AlN(CH_2C_6H_5)H$, reacts with $N(CH_2C_6H_5)H_2$ as proposed in eq 10 (K_3), subsequent sequential reactions can also be envisioned to produce the dimer. The current kinetic study does not permit us to distinguish between these two paths, but the concerted cycloaddition reaction seems more plausible, especially when the alane and amine are reacted in equal amounts. When excess benzylamine is added to a cyclopentane solution of the dimer, the unique aluminum-methyl lines of the cis/trans isomers in the ^1H NMR spectrum are lost. Only one $Al-CH_3$ line is observed, which is consistent with fast exchange. As previously mentioned, the equilibria represented by eq 10 and 12 (K_3 and K_5) are consistent with these observations.

The reaction between an alane and amine cannot be considered simple or straightforward. Many factors must influence the various steps of the reaction mechanism. As the basicity and steric effects of the amine change, many equilibria involving reactants and products are apparently introduced into the mechanism. More kinetics studies will be required to elucidate the relative importance of the different equilibria and the factors influencing the magnitude of the second-order rate constant for elimination.

Acknowledgment. This work was supported in part by the Office of Naval Research. We are indebted to Professor Gordon M. Harris for many helpful discussions on the interpretation of the kinetic data.

Registry No. $(CH_3)_2AlH$, 865-37-2; $N(CH_2C_6H_5)H_2$, 100-46-9; *cis*-$[(CH_3)_2AlN(CH_2C_6H_5)H]_2$, 77827-45-3; *trans*-$[(CH_3)_2AlN(CH_2C_6H_5)H]_2$, 77880-80-9.

Contribution from the Department of Chemistry,
Stanford University, Stanford, California 94305

N-Macrocyclic Complexes of Ruthenium(II) and Ruthenium(III)

DARREL D. WALKER and HENRY TAUBE*

Received November 5, 1980

The following new macrocycle ligand complexes of ruthenium have been synthesized: $[Ru(mac)Cl_2]Cl$ (mac = 2,3-dimethyl-1,4,8,11-tetraazacyclotetradecane (I), 1,4,8,12-tetraazacyclopentadecane (II), and 1,5,9,13-tetraazacyclohexadecane (III)). Compounds II and III, along with the previously reported $[Ru([14]aneN_4)Cl_2]Cl$ ($[14]aneN_4$ = 1,4,8,11-tetraazacyclotetradecane) comprise a series differing in the ring size of the macrocycle. Changes in ring size do not appreciably affect the charge-transfer electronic spectra or the Ru–Cl infrared stretching vibration. A small cathodic shift in the formal potential of the $Ru(mac)Cl_2^{+/0}$ couple and a decrease in the chloride affinity of the Ru(II) is observed as the ring size is increased. The structure of $[Ru([14]aneN_4)Cl_2]Br$ was determined from three-dimensional X-ray diffraction analysis, and the trans geometry of the chloro ligands was verified. Revealed in the structure are nonbonded interactions within the cation between the chloro ligands and the nitrogen-bound hydrogen atoms, which affect the charge-transfer spectra of the Ru(III) form.

Introduction

Since the discovery of the metal template synthesis by Curtis[1] and Busch[2] 20 years ago, the field of macrocyclic ligands has become a major area of research. The chemistry of first-row transition-metal ions complexed by macrocyclic ligands has been extensively developed and exhibits many unusual features compared to noncyclic analogues. The macrocycles have been shown to stabilize high oxidation states of metal ions such as Ag(II)[3] and Ni(III),[4] they exhibit unusual ligand field strengths compared to noncyclic ligands with similar donor atoms,[5] and the formation constants of their metal complexes are often unusually high (the macrocycle effect).[6]

One of the fundamental properties of these ligands is the size of the macrocycle ring. A change in ring size on high-spin, six-coordinate nickel(II)[7] and on low-spin, six-coordinate cobalt(III)[8] has been shown to affect the electronic spectra, redox potentials, and reactivity of the complexes markedly.

In an effort to extend such studies to a second-row transition-metal ion, we undertook the synthesis and characterization of a series of ruthenium macrocycle complexes. Ruthenium features two readily accessible oxidation states both of which are usually low spin and six coordinate. Additionally, its simple ammine complexes are well characterized and provide a basis for comparison to the macrocycle ligand complexes.

The ligands used in this study are shown in Figure 1 with their abbreviated names.[9] They are all fully saturated, tetraaza macrocycles, and except for $Me_2[14]aneN_4$, they lack peripheral alkyl groups. They are σ donors only and their electronic spectra will not show complications from π bonding. The series [14]-, and [15]-, and $[16]aneN_4$ provides a systematic change in the macrocycle hole size, and thus the effect of this parameter on the physical and chemical properties of the complexes may be determined. One member of the series $Ru([14]aneN_4)Cl_3$ has been reported previously.[17]

Experimental Section

Materials. $K_2[RuCl_5(OH_2)]$ was prepared from $K_3[RuCl_6]$ (Matthey-Bishop, Inc.)[10] and $K_2[RuBr_5(OH_2)]$ from ruthenium

---

(1) House, D. A.; Curtis, N. F. *Chem. Ind.* (*London*) **1961**, 1708.
(2) Blinn, E.; Busch, D. H. *Inorg. Chem.* **1968**, *7*, 820.
(3) Kestner, M. O.; Allred, A. L. *J. Am. Chem. Soc.* **1972**, *94*, 7189. Barefield, E. K.; Mocella, M. T. *Inorg. Chem.* **1973**, *12*, 2829.
(4) Gore, E. S.; Busch, D. H. *Inorg. Chem.* **1973**, *12*, 1.
(5) Busch, D. H. *Acc. Chem. Res.* **1978**, *11*, 392.
(6) Cabbiness, D. K.; Margerum, D. W. *J. Am. Chem. Soc.* **1970**, *92*, 2151.
(7) Martin, L. Y.; Sperati, C. R.; Busch, D. H. *J. Am. Chem. Soc.* **1977**, *99*, 2969.
(8) Hung, Y.; Martin, L. Y.; Jackels, S. C.; Tait, A. M.; Busch, D. H. *J. Am. Chem. Soc.* **1977**, *99*, 4029.
(9) An explanation of the derivation of the abbreviations for the macrocycle ligands may be found in the following papers: Goedken, V. L.; Merrell, P. H.; Busch, D. H. *J. Am. Chem. Soc.* **1972**, *94*, 3397. Dabrowiak, J. C.; Merrell, P. H.; Busch, D. H. *Inorg. Chem.* **1972**, *11*, 1979. The systematic names are as follows: cyclam or $[14]aneN_4$, 1,4,8,11-tetraazacyclotetradecane; $[15]aneN_4$, 1,4,8,12-tetraazacyclopentadecane; $[16]aneN_4$, 1,5,9,13-tetraazacyclohexadecane; Me_2cyclam or $Me_2[14]aneN_4$, 2,3-dimethyl-1,4,8,11-tetraazacyclotetradecane. Other abbreviations used in this paper are as follows: PPh_3, triphenylphosphine; DSS, 3-(trimethylsilyl)-1-propanesulfonic acid disodium salt; HTFMS, trifluoromethanesulfonic acid; en, ethylenediamine.
(10) Raichart, D. W. Ph.D. Thesis, Stanford University, July 1972.

0020-1669/81/1320-2828$01.25/0

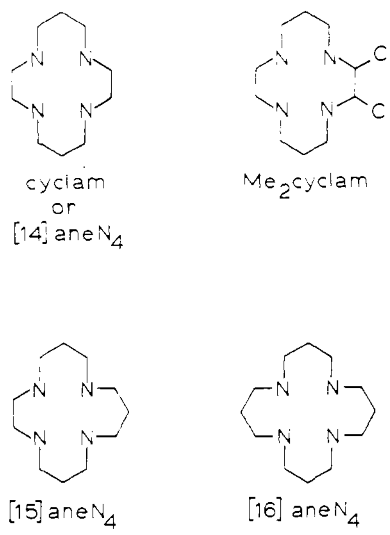

Figure 1. Structures of macrocyclic ligands.

tribromide hydrate (Engelhard Industries).[10] $RuCl_2(PPh_3)_3$ was prepared from ruthenium trichloride hydrate (Matthey-Bishop, Inc.) by Wilkinson's procedure.[11] All other chemicals were reagent grade and were used as purchased.

Reactions were carried out under argon which was deaerated by passing it through a Cr(II) scrubbing tower and dried in a concentrated H_2SO_4 tower. Water was deionized, distilled, and then redistilled from alkaline permanganate.

Ligands. [14]- and [15]aneN$_4$ were purchased from Strem Chemicals, Inc., and were not further purified. [16]aneN$_4$ was synthesized by a published procedure,[12] a higher yield synthesis of which has recently been reported.[13]

Me$_2$[14]aneN$_4$ was provided by Dr. Yann Hung and Sue Elgee of this laboratory. The free ligand was reported previously,[14] but a slightly different synthesis was used, and the physical properties were not detailed. Here, the unsaturated nickel complex[15] was reduced by using $NaBH_4$ (rather than H_2–Raney nickel), giving an 82% yield of saturated complex. The free ligand was obtained by removing nickel with cyanide ion.[16] The crude ligand was recrystallized from warm methanol–water solution to yield colorless needles (42%); mp 203–205 °C. ^{1}H NMR spectrum (60 MHz) in 20% DCl (DSS as internal standard): δ 1.5 (d, 6 H, $J \approx 6$ Hz), 2.3 (m, 4 H), 3.5 (m, 8 H), 3.7 (s, 2 H), 4.1 (m, 2 H). Anal. Calcd for $C_{12}H_{28}N_4$: C, 63.11; H, 12.36; N, 24.53. Found: C, 62.90; H, 12.28; N, 24.57.

Complexes. ***trans*-Dichloro(1,4,8,11-tetraazacyclotetradecane)ruthenium(III) chloride (*trans*-[Ru([14]aneN$_4$)Cl$_2$]Cl)** was prepared by the method of Poon,[17] except absolute ethanol was used as solvent and the reaction was allowed to proceed for 24 h under argon. The product was recrystallized from 0.1 M HCl, and then purified by using Dowex AG 50W-X2 cation-exchange resin. The UV spectrum of the eluate was monitored, and the trans isomer was separated from others, which were eluted ahead of it with 1.0 M HCl as eluant.[18] A final recrystallization from 1.0 M HCl yielded orange needles which turned to a light yellow powder when washed with acetone and dried under vacuum.

trans-[Ru([14]aneN$_4$)Cl$_2$]X where X = Br or CF_3SO_3 was prepared by dissolving the chloride salt in water and reprecipitating the cation by adding NaBr or CF_3SO_3H. The yields were greater than 90%.

Dichloro(2,3-dimethyl-1,4,8,11-tetraazacyclotetradecane)ruthenium(III) chloride monohydrate ([Ru(Me$_2$[14]aneN$_4$)Cl$_2$]Cl·H$_2$O) was obtained by the Poon method described above. $K_2[RuCl_5(OH_2)]$ (0.375 g) and ligand (0.240 g) were refluxed in 10 mL of absolute ethanol for 24 h. The solution was cooled, diluted to 50 mL with water, and cation exchanged. The yellow fraction eluted with 1.0 M HCl was evaporated to dryness and the residue recrystallized from ethanol–ether to yield orange needles. The yield was 0.228 g (51%). Anal. Calcd for $RuCl_3C_{12}H_{30}N_4O$: Ru, 22.3; Cl, 23.44; C, 31.76; H, 6.66; N, 12.35. Found: Ru, 22.5; Cl, 23.17; C, 31.71; H, 6.52; N, 12.12. The water of hydration also occurs in the CF_3SO_3 and iodide salts; its presence was verified by infrared spectroscopy.

Dibromo(1,4,8,11-tetraazacyclotetradecane)ruthenium(III) bromide ([Ru([14]aneN$_4$)Br$_2$]Br) was synthesized by refluxing 0.100 g of $K_2[RuBr_5(OH_2)]$ and 0.035 g of [14]aneN$_4$ in 10 mL of absolute ethanol for 24 h. The reaction mixture was diluted and cation exchanged with aqueous HBr as eluant. The 1.0 M HBr fraction was evaporated to dryness and the orange solid recrystallized from hot 1.0 M HBr. The yield was 0.012 g (12%). Anal. Calcd for $RuBr_3C_{10}H_{24}N_4$: C, 22.20; H, 4.47; N, 10.35. Found: C, 22.16; H, 4.43; N, 10.21.

Syntheses Using RuCl$_2$(PPh$_3$)$_3$. $RuCl_2(PPh_3)_3$ (0.5 mmol, 0.4 g) and ligand (0.5 mmol) were placed in a two-neck flask fitted with a condensor and pressure-equalizing addition funnel. Benzene (10 mL) was placed in the funnel and the entire system degassed with dry argon. The benzene was added to the solids and the mixture stirred under argon. The solids dissolved to give a dark brown solution. The air-sensitive solution was then treated under argon as described below to obtain the ruthenium complexes.

Dichloro(1,4,8,11-tetraazacyclotetradecane)(triphenylphosphine)ruthenium(II) Monohydrate (RuCl$_2$([14]aneN$_4$)(PPh$_3$)·H$_2$O). The solution above was heated for 20 h at 45 °C. The orange-yellow solid was filtered in air and recrystallized from hot methanol–water solution to yield yellow needles. The yield was 0.210 g (63%). Anal. Calcd for $RuPCl_2OC_{28}H_{41}N_4$: C, 51.53; H, 6.33; N, 8.59; Cl, 10.87. Found: C, 51.28; H, 6.25; N, 8.22; Cl, 10.26.

Dichloro(1,4,8,12-tetrazacyclopentadecane)bis(triphenylphosphine)ruthenium(II) (RuCl$_2$([15]aneN$_4$)(PPh$_3$)$_2$). The solution was stirred for 1 h at room temperature. The solid was filtered and washed with degassed benzene and ether under argon and then dried under vacuum. The resulting pink powder slowly decomposed in air. The yield was 0.153 g (34%). Anal. Calcd for $RuCl_2PC_{47}H_{56}N_4$: C, 61.97; H, 6.20; N, 6.15. Found: C, 62.15; H, 6.17; N, 6.20.

Dichloro(1,4,8,12-tetraazacyclopentadecane)ruthenium(II) (RuCl$_2$([15]aneN$_4$)). The solution was heated for 20 h at 45 °C. The resulting solid was filtered, washed with benzene and ether, and then vacuum dried. The light orange powder slowly decomposed in air. The yield was 0.137 g (71%). Anal. Calcd for $RuCl_2C_{11}H_{26}N_4$: C, 34.20; H, 6.78; N, 14.50. Found: C, 34.42; H, 6.58; N, 14.50.

Dichloro(1,5,9,13-tetraazacyclohexadecane)ruthenium(II) (RuCl$_2$([16]aneN$_4$)). The procedure was the same as for the [15]aneN$_4$ complex above. The yield was 0.131 g (65%). Anal. Calcd for $RuCl_2C_{12}H_{28}N_4$: C, 36.00; H, 7.05; N, 13.99. Found: C, 36.15; H, 7.02; N, 13.84.

Dichloro(1,4,8,12-tetraazacyclopentadecane)ruthenium(III) Chloride ([Ru([15]aneN$_4$)Cl$_2$]Cl). The solution was heated to 45 °C for 20 h, then cooled to room temperature, and after the addition of chloroform (5 mL) was heated to reflux for 4 h. The resulting solid was filtered in air, washed with benzene and ether, and then dried under vacuum. The yellow powder was cation exchanged on Dowex AG 50W-X2 resin. The 1.0 M HCl fraction was evaporated to dryness and the solid recrystallized from hot 1.0 M HCl to yield orange needles. These turned to a yellow powder when washed with acetone and dried under vacuum. The yield was 0.146 g (69%). Anal. Calcd for $RuCl_3C_{11}H_{26}N_4$: Ru, 24.0; Cl, 25.22; C, 31.22; H, 6.21; N, 13.28. Found: Ru, 24.1; Cl 24.95; C, 31.02; H, 6.09; N, 13.30.

Dichloro(1,5,9,13-tetraazacyclohexadecane)ruthenium(III) Chloride ([Ru([16]aneN$_4$)Cl$_2$]Cl). This compound was prepared as described for [Ru([15]aneN$_4$)Cl$_2$]Cl. The resulting yellow powder was recrystallized from 1.0 M HCl with LiCl added to yield orange needles. The yield was 0.050 g (23%). Anal. Calcd for $RuCl_3C_{12}H_{28}N_4$: Ru, 23.2; Cl 24.40; C, 33.07; H, 6.48; N, 12.86. Found: Ru, 23.0; Cl, 24.09; C, 33.12; H, 6.24; N, 12.74.

Equipment. ^{1}H NMR spectra were measured on a Varian Model T-60 spectrometer. UV–visible spectra were measured on a Beckman Model UV-5270 spectrophotometer. Far-infrared spectra were measured as CsI pellets on a Perkin-Elmer Model 621 spectrophotometer purged with dry nitrogen. Electrochemical measurements

---

(11) Hallman, P. S.; Stephenson, T. A.; Wilkinson, G. *Inorg. Synth.* **1970**, *12*, 237.

(12) Martin, L. Y.; Sperati, C. R.; Busch, D. H. *J. Am. Chem. Soc.* **1977**, *99*, 2968.

(13) Smith, W. L.; Ekstrand, J. D.; Raymond, K. N. *J. Am. Chem. Soc.* **1978**, *100*, 3539.

(14) Jackels, S. C.; Farmery, K.; Barefield, E. K.; Rose, N. J.; Busch, D. H. *Inorg. Chem.* **1972**, *11*, 2893.

(15) Barefield, E. K. Ph.D. Thesis, The Ohio State University, 1969.

(16) Curtis, N. F. *J. Chem. Soc.* **1964**, 2644.

(17) Chan, P. K.; Isabirye, D. A.; Poon, C. K. *Inorg. Chem.* **1975**, *14*, 2579.

(18) Isied, S. S., results submitted for publication.

Table I. Summary of Crystal Data, Intensity Collection, and Structure Refinement of *trans*-[Ru([14]aneN$_4$)Cl$_2$]Br

formula	$RuC_{10}H_{24}N_4Cl_2Br$
a, Å	7.658 (3)
c, Å	13.989 (4)
cryst system	tetragonal
V, Å^3	820.3 (4)
Z	2
ρ_{calcd}, g/cm^3	1.83
ρ_{obsd}, g/cm^3 [a]	1.85
cryst faces and dimens (from centroid), mm	(001), 0.085; $(00\bar{1})$, 0.085; (101), 0.165; $(\bar{1}0\bar{1})$, 0.165; $(10\bar{1})$, 0.165; $(\bar{1}01)$, 0.165; (011), 0.165; $(0\bar{1}\bar{1})$, 0.165; $(01\bar{1})$, 0.165; $(0\bar{1}1)$, 0.165
radiation[b]	Mo K$\bar{\alpha}$ (λ 0.071069 Å)
abs coeff μ, cm^{-1}	38.7
takeoff angle, deg	3.0
scan speed, deg/min	1.0-29.3 ($\theta/2\theta$ scans)
scan range, deg	0.8 below Kα_1 to 0.8 above Kα_1
bkgd/scan time ratio	0.25
data collected	2θ of 0-50°, *hkl*
unique av data ($F_o^2 > 3\sigma(F_o)^2$)	1023
no. of variables	65
error in observn of unit weight	1.10
R_F, %	3.0
R_{wF}, %	3.8

[a] Determined by flotation in CH_2I_2 and CCl_4. [b] Mosaic graphite monochromator.

were made with a Princeton Applied Research Model 173 potentiostat and Model 175 universal programmer system. Elemental analyses were performed by the Stanford Microanalytical Laboratory, Stanford, CA.

Crystal Data. Although the chloride salt crystallizes nicely, the crystals turn to powder on drying and thus were unsuitable for X-ray work. It was found that bromide as the counterion yielded crystals which were stable when dried, so the structure was determined on [Ru([14]aneN$_4$)Cl$_2$]Br. Suitable crystals were obtained by heating one end of a sealed tube containing solid [Ru([14]aneN$_4$)Cl$_2$]Br and water slightly acidified with HBr. The yellow crystals which formed in the cool end of the tube were truncated tetragonal bipyramids. The crystal selected was mounted on a glass fiber with epoxy cement; its faces and dimensions are listed in Table I.

Data were collected on a Syntex P2$_1$ four-circle diffractometer using graphite-monochromatized Mo K$\bar{\alpha}$ radiation. Least-squares refinement of the setting angles of 15 machine-centered reflections yielded the crystal system and unit cell dimensions (Table I). The presence of the four fold axis was confirmed by rotation photographs taken on an Enraf Nonius Diffractis 601. From the systematic absence (00*l*, $l = 2n$) two space groups were possible, $P4_2/m$ and $P4$. The centric group was indicated by a Wilson plot, and the structure was successfully refined in $P4_2/m$ with two molecules per unit cell.

Data Collection and Reduction. Examination of the ω scans of several low-angle centered reflections showed no defects in the crystal. Full peak widths at half-height were less than 0.2°. Intensity data were collected by using variable-speed 2θ-θ scans. Data collection parameters are given in Table I. Three standards were monitored every 40 reflections, and no significant change in intensity was observed. Corrections were made for background and Lorentz-polarization.[19]

Structure Solution and Refinement. The coordinates of the ruthenium and bromine atoms were determined from a three-dimensional Patterson map. The positions of the other nonhydrogen atoms were determined from subsequent difference Fourier maps. An anisotropic, full-matrix least-squares refinement of all independent nonhydrogen coordinates was performed, whereupon the locations of the hydrogen atoms were determined from another difference map. The anisotropic refinement was repeated with the hydrogen atom coordinates included as variables but with the hydrogen thermal parameters fixed and isotropic. This converged in three cycles to the final values of R_f and R_{wF} and the error in an observation of unit weight shown in Table I. A final difference Fourier map showed no maxima greater than 0.37 e/Å^3. Carbon atom peaks were 6.0 e/Å^3 or larger. Positional and thermal parameters are listed in Table II. Listings of observed and calculated structure factors (×10) and root-mean-square amplitudes of thermal vibration are available as supplementary material.

Results and Discussion

Although $K_2[RuCl_5(OH_2)]$ has been used successfully in the synthesis of numerous ruthenium amine complexes, including the 14-member ring macrocycles [14]aneN$_4$[17] and Me$_2$[14]aneN$_4$ (vida supra), it has not proven successful in the synthesis of complexes with larger macrocycle rings. Repeated experiments using Poon's synthetic method with [15]aneN$_4$ produced only small amounts of Ru(mac)Cl$_3$. The reaction solutions turn dark orange on refluxing in methanol, showing a broad absorption at approximately 480 to 490 nm. Cation exchange of the reaction solutions showed this orange product to be anionic or neutral. Elemental analysis of the orange solid indicated two chlorides per ruthenium macrocycle (calcd 18.5; (2Cl), 25.2% (3Cl); found 18.6%). In addition, the infrared spectrum showed a moderately strong band at 1615 cm^{-1}. These observations strongly indicate the orange product is a ruthenium(II) imine complex. The dehydrogenation of ruthenium complexes of primary amines is a well-known reaction.[20]

It should also be noted that Poon's synthesis produces variable amounts of the cis isomer which is not removed by recrystallization from hydrochloric acid.[18] The substitution of the higher boiling ethanol for methanol reduces the amount of the cis isomer to less than 10% of the total yield. However, the subsequent purification by cation exchange is still necessary.

After investigating several ruthenium compounds as starting materials, we found that the reaction of RuCl$_2$(PPh$_3$)$_3$ with the larger macrocycles in benzene gave good yields of the desired products without formation of the imine complex. The replacement of PPh$_3$ by the macrocycle probably proceeds in a stepwise fashion since an intermediate product which contains two PPh$_3$ ligands can be isolated when [15]aneN$_4$ is the macrocycle. This intermediate complex was isolated in analytically pure form, but no attempt was made to characterize it further. For both [15]- and [16]aneN$_4$, the reaction proceeds rapidly to form the Ru(mac)Cl$_2$ complex when the reaction solution is slightly heated. The same reaction conditions using the smaller cyclam ligand yields a product which contains a single PPh$_3$ (analysis corresponds approximately to RuCl$_2$([14]aneN$_4$)PPh$_3$). However, even refluxing in toluene fails to cause displacement of the final PPh$_3$. The monophosphine product is also formed with the methyl-substituted 14-member ring, Me$_2$[14]aneN$_4$. The ease with which PPh$_3$ is displaced from ruthenium seems to depend more on the ring size of the macrocycle than on the bulk of the ligand and qualitatively falls in the order [14]aneN$_4$ << [15]aneN$_4$ < [16]aneN$_4$.

Description of Structure. Certain unusual aspects of the electronic and infrared spectra of the cyclam complex (vida infra) led us to undertake the determination of its crystal structure to verify the trans-geometry assignment of Poon.

Figure 2 is a schematic representation of the cation and shows the atom numbering scheme, bond distances, and bond angles. Figure 3 is an ORTEP view of the cation with the hydrogen atoms included. The chloride ligands are trans to each other as in the original assignment, and the cation has

---

(19) In addition to the local data reduction program ENXDR, the programs used included full-matrix least squares and Fourier programs and Johnson's ORTEP. All calculations were carried out on a PDP 11/45 computer. Atomic scattering factors were taken from: "International Tables for X-ray Crystallography"; Kynoch Press: Birmingham, England, 1974; Vol. IV.

(20) For example, see: Mahoney, D. F.; Beattie, J. K. *Inorg. Chem.* **1973**, *12*, 2561. Diamond, S. E.; Tom, G. M.; Taube, H. *J. Am. Chem. Soc.* **1975**, *97*, 2661.

Table II. Positional and Thermal Parameters for *trans*-[Ru([14]aneN$_4$)Cl$_2$]Br

atom	position	site symmetry	x	y	z	occupancy	B^a or β_{11}	β_{22}	β_{33}	β_{12}	β_{13}	β_{23}
Ru	c	$2/m$	0	$^1/_2$	0	0.25	1.92 (1)	1.69 (1)	2.37 (1)	0.29 (2)	0	0
Br	e	$\bar{4}$	0	0	$^1/_4$	0.25	3.10 (3)	β_{11}	3.86 (3)	0	0	0
Cl	j	m	0.2382 (1)	0.3078 (1)	0	0.5	2.59 (4)	2.71 (4)	4.63 (5)	0.87 (3)	0	0
N	k	1	0.1057 (3)	0.6468 (3)	0.1112 (2)	1.0	3.1 (1)	2.59 (9)	3.4 (1)	0.52 (9)	−0.62 (9)	−0.25 (9)
C1	k	1	0.0898 (6)	0.5419 (5)	0.1998 (3)	1.0	6.3 (2)	3.7 (1)	2.9 (1)	1.2 (2)	−1.3 (1)	−0.5 (1)
C2	k	1	0.2837 (5)	0.7153 (5)	0.0924 (3)	1.0	3.1 (1)	3.8 (1)	6.3 (2)	−0.1 (1)	−1.6 (1)	−1.1 (2)
C3	j	m	0.2923 (7)	0.8177 (7)	0	0.5	3.1 (2)	2.8 (2)	7.6 (3)	−0.6 (2)	0	0
H1(N)	k	1	0.039 (5)	0.735 (5)	0.118 (3)	1.0	5.0					
H1(C1)	k	1	0.186 (5)	0.450 (5)	0.194 (3)	1.0	5.0					
H2(C1)	k	1	0.102 (5)	0.612 (5)	0.252 (3)	1.0	5.0					
H1(C2)	k	1	0.375 (5)	0.618 (5)	0.092 (3)	1.0	5.0					
H2(C2)	k	1	0.316 (5)	0.785 (5)	0.152 (3)	1.0	5.0					
H1(C3)	j	m	0.392 (7)	0.878 (7)	0	0.5	5.0					
H2(C3)	j	m	0.189 (7)	0.908 (8)	0	0.5	5.0					

^{a} In Å^2.

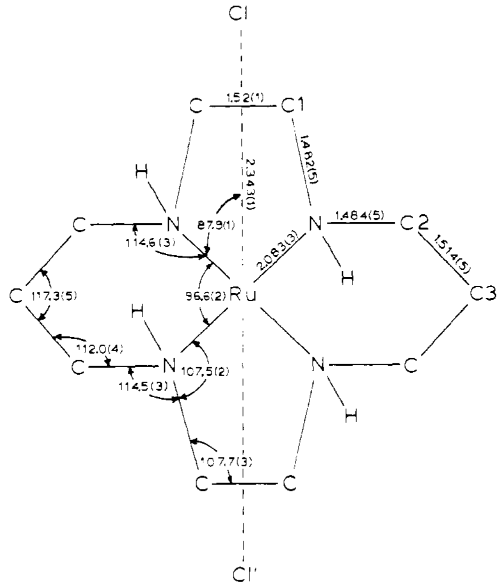

Figure 2. Atom numbering scheme, bond distances, and bond angles in *trans*-Ru([14]aneN$_4$)Cl$_2$$^+$.

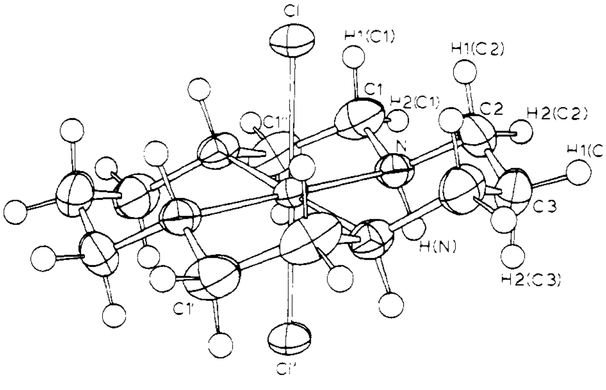

Figure 3. ORTEP view of the cation, including hydrogen atoms.

overall C_{2h} symmetry. The two 6-member chelate rings are in chair conformations and the two 5-member rings are in gauche conformations. The overall structure of the cation is the trans-III isomer of Tobe,[21] with two adjacent N–H hydrogen atoms directed toward one side of the macrocycle plane and the other two directed toward the opposite side of the plane. This is presumed to be the most stable configuration for otherwise unhindered 14-member ring macrocycles and has also been found in the [14]aneN$_4$ complexes of nickel(II),[22] cobalt(III),[23] and copper(II).[24]

Table III. Selected Nonbonded Distances within the Cation *trans*-Ru([14]aneN$_4$)Cl$_2$$^+$

nonbonded pair	dist, Å
Cl′–H(N)	2.71 (4)
Cl–H1(C1)	2.95 (4)
Cl–H1(C2)	3.23 (4)
Cl′–H2(C3)	3.08 (6)

Bond distances within the cation are not unusual. The ruthenium–nitrogen distance of 2.083 (3) Å is slightly shorter than in the tris(ethylenediamine)ruthenium(III) complex (2.11 Å)[25] or hexaammineruthenium(III) (2.104 Å)[26] and may reflect a small contraction due to the small hole size of cyclam. Bond distances and angles within the chelate rings correspond closely to the same measurements in the cobalt and copper complexes and are little different from those found in the structure of [cyclamH$_2$](ClO$_4$)$_2$.[27]

A significant distortion from square-planar coordination is observed for the four nitrogen atoms. Although the symmetry of the structure requires the nitrogens to be strictly planar with the ruthenium, the angles subtended by the chelate rings deviate from 90° in a manner consistent with the number of atoms in the ring. Bond angles less than 90° are observed for 5-member rings (83.4 (2)° in this structure) and angles greater than 90° are observed for 6-member rings (96.6 (2)°). This corresponds to a distortion of the square coordination geometry in the equatorial plane producing a rectangle with sides of 2.770 (6) and 3.111 (6) Å (see Figure 2). The angular distortions in this structure are 2.3 to 2.6° larger than in the complexes of first-row metal ions, reflecting the slightly longer metal–nitrogen bond distance.

Nonbonded interactions within the cation cause a further distortion from a regular octahedral arrangement of ligating atoms. The Cl–Ru–Cl axis is not perpendicular to the equatorial plane but is tilted slightly toward H(N) atoms and away from H(C) atoms. These nonbonded distances are listed in Table III. The Cl′–H(N) distance of 2.7 Å is somewhat shorter than the sum of the van der Waals radii (3.0–3.3 Å)[28]

---

[21] Bosnich, G.; Poon, C. K.; Tobe, M. L. *Inorg. Chem.* **1965**, *4*, 1102.

[22] Bosnich, B.; Mason, R.; Pauling, P. J.; Robertson, G. B.; Tobe, M. L. *Chem. Commun.* **1965**, 97.

[23] Endicott, J. F.; Lilie, J.; Kuszaj, J. M.; Ramaswamy, B. S.; Schmonsees, W. G.; Simic, M. G.; Glick, M. D.; Rillema, D. P. *J. Am. Chem. Soc.* **1977**, *99*, 429.

[24] Taskar, P. A.; Sklar, L. *Cryst. Mol. Struct.* **1975**, *5*, 329.

[25] Peresie, H. J.; Stanko, J. A. *Chem. Commun.* **1970**, 1674.

[26] Stynes, H. C.; Ibers, J. A. *Inorg. Chem.* **1971**, *10*, 2304.

[27] Nave, C.; Truter, M. R. *J. Chem. Soc., Dalton Trans.* **1974**, 2351.

Table IV. Electronic Spectral Data for Ruthenium Macrocycle and Related Complexes

complex	λ_{max}, nm ($10^{-3}\epsilon$, M^{-1} cm^{-1})
trans-$[Ru([14]aneN_4)Cl_2]Cl$[a]	358 (2.56), 315 (1.23)
trans-$[Ru([15]aneN_4)Cl_2]Cl$	359 (2.41), 317 (1.35)
trans-$[Ru([16]aneN_4)Cl_2]Cl$	360 (2.32), 318 (1.32)
trans-$[Ru(Me_2[14]aneN_4)Cl_2]Cl\cdot H_2O$	359 (2.43), 316 (1.26)
trans-$[Ru([14]aneN_4)Br_2]Br$	431 (3.39), 355 (0.49)
trans-$[Ru(NH_3)_4Cl_2]Cl$[b]	331 (5.0), 295 sh (0.70)
cis-$[Ru(NH_3)_4Cl_2]Cl$[b]	350 (1.5), 308 (1.3), 262 (0.5)
trans-$[Ru(en)_2Cl_2]Cl$[c]	343 (3.85), 292 sh (0.80), 272 (0.90)
cis-$[Ru(en)_2Cl_2]Cl$[c]	354 (1.75), 314 (1.42), 269 (0.90)

[a] Reference 1 reports the following values: 357 (2.26), 312 (1.25). [b] Reference 2. [c] Reference 1.

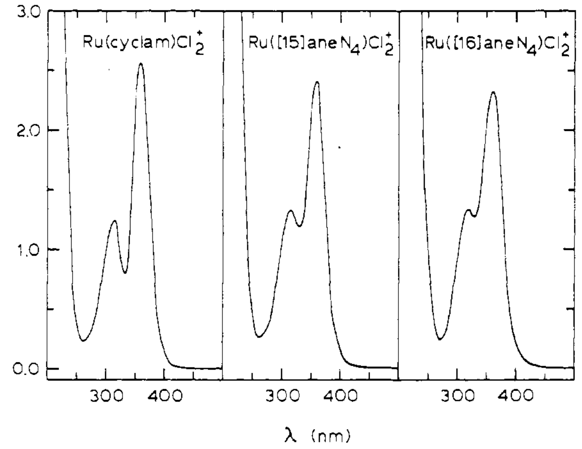

Figure 4. UV spectra of $Ru(mac)Cl_2^+$ complexes.

and indicates that there is a significant attraction between the two atoms. The hydrogen atoms were located directly from peaks in a difference Fourier map and their position parameters were successfully included in the last cycles of least-squares refinement. Bonding distances for the hydrogens ranged from 0.85 to 1.05 Å, and no large distortions from tetrahedral bond angles were observed. Small increases in the N-H bond length (0.1–0.2 Å) do not significantly change the Cl-H(N) distance.

Electronic Spectra. A summary of electronic spectral data for the macrocycle and related complexes is given in Table IV. The two-band spectrum of the $[14]aneN_4$ complex is typical of the macrocycle series (see Figure 4). The major difference in the spectra as the macrocycle ring size increases is a loss of depth in the minimum between the two peaks. The most striking feature of these spectra is the presence of two strong absorption bands rather than the single strong band observed in the structurally similar *trans*-dichlorotetraammine- and *trans*-dichlorobis(ethylenediamine)ruthenium(III) complexes (see Table IV). The spectra of the macrocycle complexes more closely resemble those of the corresponding *cis*-isomers in both the position and intensity of the bands. It was this anomaly and certain features of the infrared spectra of these complexes (vida infra) which led us to determine the crystal structure of the cyclam complex.

The electronic spectra of *cis*- and *trans*-dichlorotetraammineruthenium(III) complexes have been assigned previously.[29] The spectra are dominated by ligand to metal

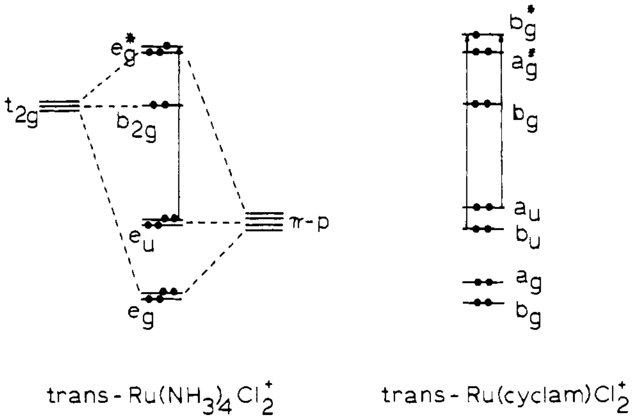

Figure 5. Simplified molecular orbital diagram for ruthenium(III) complexes.

Table V. Far-Infrared Spectral Data for the Ruthenium(III) Macrocycle and Related Complexes (350–200 cm^{-1})

	bands, cm^{-1}	
compd	M-X (str)	δ_{NMN} and π_{NMN}
trans-$Ru(NH_3)_4Cl_2^+$[a]	323	225
cis-$Ru(NH_3)_4Cl_2^+$[b]	310, 285	258
$Ru([14]aneN_4)Cl_2^+$	321	299, 240
$Ru([14]aneN_4)Br_2^+$	213	249
$Ru(Me_2[14]aneN_4)Cl_2^+$	331	301, 255
$Ru([15]aneN_4)Cl_2^+$	321	299
$Ru([16]aneN_4)Cl_2^+$	323	264

[a] Reference 31. [b] Reference 32.

charge-transfer bands corresponding to the transfer of an electron from a filled chloride p–π orbital to the lowest unoccupied d orbital on ruthenium (see Figure 5a). For the trans isomer (D_{4h} symmetry) a single Laporte-allowed transition is predicted, corresponding to the most intense absorption in the electronic spectra of *trans*-dichlorotetraammmine- and *trans*-dichlorobis(ethylenediamine)ruthenium(III) complexes at 331 and 343 nm, respectively. For this cis isomer, the symmetry is lower and the chloride p–π orbitals no longer occur in degenerate pairs. The *cis*-dichlorotetraammineruthenium(III) complex has C_{2v} symmetry which has a similar energy level to C_{2h} shown in Figure 5b, but will lack the g and u designations. Two absorptions are expected, corresponding to the two most intense bands in the spectra of the cis complexes (see Table IV).

The splitting in the spectra of the *trans*-$Cl_2(mac)Ru^{III}$ complexes is attributed to the interaction between the chloride ligands and the hydrogen atoms attached to nitrogens (vida supra). This interaction splits the degeneracy of the chloride p–π levels producing two Laporte-allowed transitions (Figure 5b). The metal centered e_g* orbitals are also split due to the rectangular distortion of equatorial plane but will have no effect on the number of allowed transitions.

It is observed that changes in the macrocycle ring size have almost no effect on the electronic spectra of these complexes. This contrasts with the large differences observed as the ring size changes in complexes of first-row transition metals.[30] However, it must be remembered that we are dealing here with charge transfer rather than d–d transitions as in the case of most of the spectrophotometric data for the first-row transition elements. For the latter, relatively large differences arise from the direct interaction of macrocycle donor atoms with the metal σ–d orbitals so that small differences in ring size will have

---

(28) Pauling, L. "The Nature of the Chemical Bond", 3rd ed.; Cornell University Press: Ithaca, New York, 1960; p 260.

(29) Verdonck, E.; Vanquickenborne, L. G. *Inorg. Chem.* **1974**, *13*, 762.

(30) Martin, L. Y.; DeHayes, L. J.; Zompa, L. J.; Busch, D. H. *J. Am. Chem. Soc.* **1974**, *96*, 4046.

Table VI. Electrochemical Data for $Ru^{II/III}$ Couple in Ruthenium Macrocycle and Related Complexes

	$E_{1/2}$ (vs. NHE), mV			
ligands	X_2 = Cl_2	X_2 = $(Cl)(H_2)$	X_2 = $(H_2)_2$	X_2 = Br_2
trans-([14]aneN_4)X_2	−150	−15	+155	−95
trans-(Me_2[14]aneN_4)X_2	−155	0	+135	
trans-([15]aneN_4)X_2	−125	+35	+190	
trans-([16]aneN_4)X_2	−95	+65	+225	
trans-$(NH_3)_4Cl_2$[a]	−164	−70	+46	
trans-$(en)_2Cl_2$[b]	−188	−66	+92	

[a] Reference 38. [b] Reference 39.

strong effects on the d–d splittings. In the charge-transfer spectra of ruthenium(III) complexes, the metal d orbitals of interest are of π symmetry and do not interact strongly with the macrocycle nitrogens. Hence, changes in the ring size would not be expected to alter the spectra significantly.

Infrared Spectra. The far-infrared spectra (350–200 cm^{-1}) were measured in order to assign the Ru–Cl stretching vibrations. The results are shown in Table V. Typically, Ru(III)–Cl stretching vibrations are found between 330 and 270 cm^{-1} when the other ligands are saturated nitrogen donors.[31,32] For the *trans*- and *cis*-dichlorotetraammineruthenium(III) complexes, group theoretical analysis predicts, respectively, one and two infrared-active metal–halide stretching vibrations. These are observed at 323 cm^{-1} (trans)[32] and at 310 and 255 cm^{-1} (cis).[31]

Spectra of the macrocycle complexes showed two bands in the region. The absorption near 325 cm^{-1} is assigned to the Ru–Cl asymmetric stretch and corresponds closely in energy to the same vibration in *trans*-$[Ru(NH_3)_4Cl_2]Cl$.

This assignment is supported by the spectrum of the bromo complex [Ru([14]aneN_4)Br_2]Br, which was synthesized in a manner analogous to the chloro complex. Substituion of bromine for chlorine moves the ruthenium–halide stretch to lower energy (213 cm^{-1}), resulting in the observed loss of the 332-cm^{-1} band. The trans geometry of the bromo complex is ensured by the similarity of its infrared spectrum to that of the chloro complex in the CH_2 rocking region (900–800 cm^{-1}). In this region, both complexes show the distinctive three-band spectra expected for (*trans*-dihalocyclam)metal complexes.[33]

In the region 350–200 cm^{-1}, bands corresponding to in-plane (δ_{NMN}) and out-of-plane (π_{NMN}) deformation modes are found.[31,33] These are listed in Table VI (the assignments should be taken as tentative). Of these, the absorptions near 300 cm^{-1} in the cyclam and [15]aneN_4 complexes deserve further comment. In view of the loss of this band in [Ru([14]aneN_4)Br_2]Br, we originally thought it was the symmetric Ru–Cl stretch, made active through solid-state interactions. The crystal structure, though, shows the solid has a center of inversion at the ruthenium atom, so the symmetric stretch still should not become infrared active. This band could also be due to a low-energy lattice vibration. However, the band occurs almost unchanged in intensity and location whether the anion in the solid is chloride, bromide, perchlorate, or fluoroborate, thus eliminating this as a probable cause.

Electrochemistry. Cyclic voltammograms of the macrocycle complexes were measured, and the results are shown in Table VI. As the macrocycle ring size increases, the formal potential (E_f) of the $Ru^{III/II}$ couple becomes more positive, indicating an increase of the stability of Ru(II) species over the Ru(III).

Table VII. Chloride Affinity Constants for Ruthenium(II) Macrocycle Complexes

complex	K_1[a]	K_2[b]
$Ru(NH_3)_5(H_2O)$	1.6[c]	
Ru([14]aneN_4)$(H_2O)_2$	32	9
Ru(Me_2[14]aneN_4)(H_2O)	21	4.5
Ru([15]aneN_4)$(H_2O)_2$	10	3
Ru([16]aneN_4)$(H_2O)_2$	9	3

[a] K_1 = [monochloro]/[aquo][Cl^-] (standard state, M). [b] K_2 = [dichloro]/[monochloro][Cl^-] (standard state, M). [c] Reference 36.

This trend is expected since the slightly larger Ru(II) ion should be more easily accommodated in the macrocycle as the ring size increases. Changes in solvation energies will also increase the stability of the lower charged species as the hydrocarbon content of the macrocycle increases, thus also contributing to the observed trend in E_f. The overall effect, a change of 55 mV between [14]- and [16]aneN_4 is relatively small compared to the 580-mV change in the same series of cobalt complexes.[35] The small effect seen in the ruthenium complexes reflects the fact that the electron involved in the reduction enters a nonbonding π–d orbital and its energy is little affected by the macrocycle ligand. In contrast, in the cobalt series, the electron enters an antibonding σ–d orbital whose energy is very sensitive to the macrocycle ring size.

The reversibility of the $Ru^{III/II}$ couple decreases as the macrocycle ring size increases. For $[Ru([14]aneN_4)Cl_2]^+$ at 100 mV s^{-1} scan rate, the peak-to-peak separation is 59 mV and the ratio of anodic to cathodic currents is 0.99 in 0.1 M HCl and only slightly less in 0.1 M CF_3SO_3H. Similar behavior, though with slightly lower current ratios, is observed for the [15]aneN_4 complex. However, at such slow scan rates the $Ru([16]aneN_4)Cl_2^+$ spectrum is irreversible. Much faster scan rates (5 V/s) reveal the anticipated oxidation wave 59 mV more positive than the reduction wave and a second wave at more positive potentials. This behavior is due to the aquation of the dichloro complex in the reduced state to form the chloroaquo ion. Longer reduction times produce a third set of peaks due to the diaquo ion. The rate of loss of chloride has been determined from the cyclic voltammograms and will be reported in a subsequent paper on the reactivity of these complexes.

Chloride Affinity. During the investigation of solutions of the ruthenium(II) macrocycle complexes in chloride media, an unexpectedly high affinity for chloride was observed. In order to assess this quantitatively, we made polarographic measurements to determine the relative amounts of the various species in solution. The equilibria involved are

$$Ru(mac)(H_2O)_2^{2+} + Cl^- \underset{}{\overset{K_1}{\rightleftharpoons}} Ru(mac)(H_2O)(Cl)^+ + H_2O \quad (1)$$

$$Ru(mac)(H_2O)(Cl)^+ + Cl^- \overset{K_2}{\rightleftharpoons} Ru(mac)(Cl)_2 + H_2O \quad (2)$$

The values of K_1 and K_2 given in Table VII are averages determined from solutions with differing chloride concentrations.

All the macrocycle complexes show increased affinity for chloride compared to the simpler ammine complexes. A large increase in affinity is observed for the cyclam complex over the $Ru(NH_3)_5(H_2O)^{3+}$ ion,[36] but a decrease is observed as

---

(31) Broomhead, J.; Kane-Maguire, L.A.P. *J. Chem. Soc. A.* **1967**, 546.

(32) Broomhead, J. A.; Kane-Maquire, L.A.P.; Wilson, D. *Inorg. Chem.* **1975**, *14*, 2575.

(33) Poon, C. K. *Inorg. Chim. Acta.* **1971**, *5*, 322.

(34) Hung, Y. Ph.D. Thesis, The Ohio State University, 1975.

(35) Hung, Y.; Martin, L. Y.; Jackels, S. C.; Tait, A. M.; Busch, D. H. *J. Am. Chem. Soc.* **1977**, *94*, 4029.

(36) Lim, H. S.; Barclay, D. J.; Anson, F. C. *Inorg. Chem.* **1972**, *11*, 1460.

(37) Kuehn, C. G.; Taube, H. *J. Am. Chem. Soc.* **1976**, *98*, 689.

(38) Isied, S. S.; Taube, H. *Inorg. Chem.* **1976**, *15*, 3070.

(39) Poon, C. K.; Che, C. M. *J. Chem. Soc., Dalton Trans.* **1980**, 756.

methyl or methylene groups are added to the macrocycle. Again, increasing the bulk of the ligand will favor the lower charged chloro complexes over the aquo species through solvation effects, thus contributing to the observed increase in chloride affinity for the macrocycle complexes. The decrease with increasing ring size is probably due to steric interactions between the axial positions and the various hydrogen atoms on the macrocyclic ring. The crowding caused by the hydrogen atoms will tend to displace the larger chloride ligand in favor of the smaller aquo ligand.

Summary

The most unusual aspect of the ruthenium macrocycle complexes compared to the simple ammine systems is the appearance of effects due to steric interactions between the macrocycle ligand and the axial positions. These interactions are directly observable in the crystal structure and lead to the splitting of the charge-transfer band in the electronic spectrum. This interaction is also apparent in the decreasing affinity for chloride as the macrocycle ring size increases.

Other trends seen in the properties of the macrocycle complexes are consistent with solvation effects as chelation is increased or as the ring size is increased. The effects of ring size on the electronic spectra and formal potentials are found to be small, as might be expected because there are no e_g electrons.

Acknowledgment. Support of this research by the National Science Foundation under Grant No. CHE79-08633 and the National Institutes of Health (Grant No. GM 13638-14) is gratefully acknowledged as is the help of Proessor K. O. Hodgson and Jeremy Berg in determining the crystal structure.

Registry No. *trans*-[Ru([14]aneN$_4$)Cl$_2$]Cl, 56172-98-6; *trans*-[Ru([14]aneN$_4$)Cl$_2$]Br, 77827-63-5; *trans*-[Ru([14]aneN$_4$)Cl$_2$]CF$_3$SO$_3$, 77827-64-6; *trans*-[Ru(Me$_2$[14]aneN$_4$)Cl$_2$]Cl, 77827-65-7; *trans*-[Ru([14]aneN$_4$)Br$_2$]Br, 74202-83-8; RuCl$_2$([14]aneN$_4$)(PPh$_3$), 77827-66-8; RuCl$_2$([15]aneN$_4$)(PPh$_3$)$_2$, 77846-74-3; RuCl$_2$([15]aneN$_4$), 77827-67-9; RuCl$_2$([16]aneN$_4$), 77827-68-0; *trans*-[Ru[15]aneN$_4$)Cl$_2$]Cl, 76705-25-4; *trans*-[Ru([16]aneN$_4$)Cl$_2$]Cl, 77827-69-1; *trans*-[Ru([14]aneN$_4$)Cl(H$_2$O)]$^+$, 73238-31-0; *trans*-[Ru(Me$_2$[14]aneN$_4$)Cl(H$_2$O)]$^+$, 77827-70-4; *trans*-[Ru([15]aneN$_4$)Cl(H$_2$O)]$^+$, 77827-71-5; *trans*-[Ru([16]aneN$_4$)Cl(H$_2$O)]$^+$, 77827-72-6; *trans*-[Ru([14]aneN$_4$)(H$_2$O)$_2$]$^{2+}$, 77827-73-7; *trans*-[Ru(Me$_2$[14]aneN$_4$)(H$_2$O)$_2$]$^{2+}$, 77827-74-8; *trans*-[Ru([15]aneN$_4$)(H$_2$O)$_2$]$^{2+}$, 77827-75-9; *trans*-[Ru([16]aneN$_4$)(H$_2$O)$_2$]$^{2+}$, 77846-75-4; K$_2$[RuCl$_5$(OH$_2$)], 14404-33-2; K$_2$[RuBr$_5$(OH$_2$)], 62109-80-2; RuCl$_2$(PPh$_3$)$_3$, 15529-49-4; Me$_2$[14]aneN$_4$, 39481-23-7.

Contribution from the Evans Chemical Laboratory,
The Ohio State University, Columbus, Ohio 43210

Simultaneous Synthesis, Separation, and Characterization of Metal Complexes with Monomeric Lacunar Ligands and Dimeric Ligands Capable of Bimetallic Coordination

DARYLE H. BUSCH,* SUSAN C. JACKELS, ROBERT C. CALLAHAN, JOSEPH J. GRZYBOWSKI,
L. LAWRENCE ZIMMER, MASAAKI KOJIMA, DENNIS J. OLSZANSKI, WAYNE P. SCHAMMEL,
JAMES C. STEVENS, KATHERINE ANNE HOLTER, and JAN MOCAK

Received December 10, 1980

Two important families of ligands are produced simultaneously in a template-moderated ring-closure reaction. Additional examples of lacunar ligands are reported; these form metal complexes in which a protected cavity suitable for sheltering a small molecule is formed in the vicinity of a coordination site. Simultaneously, dimeric ligands are produced that are capable of binding two metal ions, within macrocyclic moieties, in an approximate face-to-face orientation. The isomeric substances were separated by fractional crystallization or by chromatography. Their structures have been established by combination of definitive and correlative means. Generic distinctions between monomers and dimers are made by high-performance liquid and ion-exchange chromatography, by NMR (proton and ^{13}C), and, in some cases, by direct molecular weight determinations on neutral deprotonated derivatives of the nickel(II) complex. Factors favoring monomer and dimer formation are discussed. The monomeric species are the main subject of this paper. ^{13}C NMR show that most of the lacunar complexes have the expected mirror symmetry. Electrochemistry shows that the electron density at the metal ion is insensitive to the nature of the bridge but that substituents can cause alterations in electon density. Thus steric and electronic effects of variations in ligand can be applied separately to the interactions of small molecules such as O$_2$ or CO with coordinated metal ions. The ligands have been separated from nickel(II) and made available for coordination to other metal ions.

Introduction

Structural variations are being explored for the broad family of bicyclic superstructure complexes shown in structure I. The general structure has been designed for use in various totally synthetic heme protein models. Preliminary reports[1,2] have revealed the synthesis and structure proof for examples of the new complexes. They have also shown that the cobalt(II) complexes of these lacunar ligands are exceptional O$_2$ carriers:[3] (1) the O$_2$ affinity of the *lacunar*-cobalt(II) complexes can be made to vary over a range of 5 orders of magnitude by steric means; (2) electronic effects can be used to change the O$_2$ affinity by at least 1 order of magnitude; (3) the O$_2$ complexes are formed reversibly in aqueous solution at room temperature; (4) certain of the *lacunar*-cobalt complexes have O$_2$ affinities as great as those of iron in myoglobin and are the strongest reversible cobalt-based O$_2$ binders known to react in a one-to-one stoichiometry.[4]

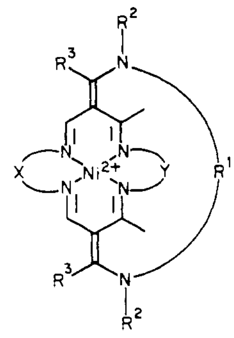

I

---

[1] Schammel, W. P.; Mertes, K. S. B.; Christoph, G. G.; Busch, D. H. *J. Am. Chem. Soc.* **1979**, *101*, 1622–1623.

[2] Stevens, J. C.; Jackson, P. J.; Schammel, W. P.; Christoph, G. G.; Busch, D. H. *J. Am. Chem. Soc.* **1980**, *102*, 3283–3285.

[3] Stevens, J. C.; Busch, D. H. *J. Am. Chem. Soc.* **1980**, *102*, 3285–3287.

0020-1669/81/1320-2834$01.25/0